Analysis of a Metastable Electronic Excited State of Sodium Nitroprusside by X-ray Crystallography

Mark R. Pressprich,* Mark A. White, Yanina Vekhter, and Philip Coppens*

Contribution from the Department of Chemistry, State University of New York at Buffalo, Buffalo, New York 14214-3094

Received November 29, 1993⊛

Abstract: The structure and electron density distribution of the electronic ground state and an electronic excited state of $Fe(CN)_5(NO)^{2-}$ in crystalline sodium nitroprusside dihydrate, $Na_2[Fe(CN)_5NO]\cdot 2H_2O$, have been determined from X-ray diffraction data at 138 K. The statistically significant geometrical distortions ($\Delta_i > 3\sigma(\Delta_i)$) of metastable state I are an elongation of the Fe–N bond by 0.049(8) Å from 1.668(1) Å to 1.717(8) Å and a decrease in the average *cis* ∠N–Fe–C angle by 0.8(2)° from 95.51(3)° to 94.75(19)°. The decrease in the ∠N–Fe–C angle is understood as a minimization of ligand–ligand repulsion, which leaves the average axial to equatorial ligand distances essentially unchanged. No significant increase in bending of the Fe–N–O angle is observed. Analysis of the diffraction data with the multipole electron density formalism shows a significant decrease of the d_{xy} electron density on the metal atom, which indicates that metastable state I (MS_I) arises from partial depopulation of the ground-state HOMO. The results, combined with information from previously reported polarization studies, suggest that MS_I and MS_{II} are relaxed derivatives of the excited configurations a′ $(2b_2)^1a''$ $(7e)^1$ and a′ $(2b_2)^1a'$ $(7e)^1$.

Introduction

Recently, four transition-metal nitrosyl complexes have been found to exhibit extremely long-lived electronic excited states following photoexcitation with wavelengths of $350 < \lambda < 580$ nm. The most studied of these is the nitroprusside anion, $Fe(CN)_5(NO)^{2-}$, for which either one or two metastable states have been found depending on the cation and its environment in solution, glass or crystal.[1] The photostationary excited-state population is wavelength and polarization dependent but is always less than 50%,[2] so physical measurements of the excited state are necessarily performed on mixed-state crystals. Two metastable states have also been found upon irradiation of crystalline $K_2[Ru(NO_2)_4(OH)(NO)]$ and $K_2[RuCl_5(NO)]$,[3] while only one metastable state is known for Ni Cp(NO) (Cp = η^5-cyclopentadienyl).[4] In crystalline sodium nitroprusside dihydrate (SNP) metastable state I (MS_I) and metastable state II (MS_{II}) have lifetimes greater than 10^4 s at temperatures below 185 and 140 K, respectively.[5] Nitroprusside salts have therefore been suggested for use as optical storage devices.[6,7] Calorimetry and Raman experiments show that MS_I and MS_{II} lie 1.1 and 1.0 eV, respectively, above the ground state.[5]

The wavelength dependence of the formation of the SNP metastable states indicates the states to be a relaxed byproduct of the charge-transfer transition $3d \rightarrow \pi^*(NO)$. According to molecular orbital calculations (in which C_{4v} symmetry is assumed), the orbitally degenerate (e) LUMO has primarily $\pi^*(NO)$, d_{xy} and d_{yz} character and is totally antibonding.[8-11] Vibrational spectroscopy supports the association of the SNP metastable states with the promotion of an electron to the totally antibonding ground-state LUMO. The ground-state $\nu(NO)$ stretching frequency decreases from 1950 to 1835 cm^{-1} for MS_I and to 1663 cm^{-1} for MS_{II}, while $\nu(Fe–N)$ decreases from 658 cm^{-1} to 565 and 547 cm^{-1} for MS_I and MS_{II}, respectively.[12]

In order to directly determine the geometry and electronic nature of one of the two metastable states (MS_I), we have analyzed photoexcited crystals of SNP by X-ray diffraction. Preliminary results have been reported.[13] We report here the complete X-ray structural analysis and the new electron density study of the MS_I state. To our knowledge, this is the first electron density study of any electronically excited material.

The average geometries of the ground and MS_I and ground and MS_{II} excited states have been determined in a previous series of neutron diffraction studies.[14,15] The results support the spectroscopic conclusions and confirm the elongation of the Fe–N bond. A quantitative measure of the SNP distortion was obtained by assuming the actual distortions Δ_i^{actual} to be related to the differences between the average and ground-state structures $\Delta_i^{measured}$ by the linear expression

$$\Delta_i^{actual} = \Delta_i^{measured}/p^{excited} \quad (1)$$

where $p^{excited}$ is the fractional excited population. In the present study a scattering formalism is used which explicitly includes the scattering of both the ground and excited states.

A recent set of excited-state Raman experiments on SNP raises additional questions which are addressed here. Stretching

* Authors to whom correspondence should be addressed.

⊛ Abstract published in *Advance ACS Abstracts*, May 15, 1994.

(1) Zöllner, H.; Krasser, W.; Woike, T. *Chem. Phys. Lett.* **1989**, *161*, 497–501.
(2) Hauser, U.; Oestreich, V.; Rohrweck, H. D. *Z. Phys.* **1977**, *A280*, 17–25.
(3) Woike, T.; Zöllner, H.; Krasser, W.; Haussühl, S. *Solid State Commun.* **1990**, *73*, 149–152. Woike, T.; Haussühl, S. *Solid State Commun.* **1993**, *86*, 333–337.
(4) Crichton, O.; Rest, A. J. *J. Chem. Soc., Dalton Trans.* **1977**, *10*, 986–993.
(5) Zöllner, H.; Woike, T.; Krasser, W.; Haussühl, S. *Z. Kristallogr.* **1989**, *188*, 139–153.
(6) Woike, T.; Krasser, W.; Bechthold, P.; Haussühl, S. *Phys. Rev. Lett.* **1984**, *53*, 1767–1770.
(7) U.S. patent No. 4,713,795.
(8) Manoharan, P. T.; Gray, H. B. *J. Am. Chem. Soc.* **1965**, *87*, 3340–3348. Manoharan, P. T.; Gray, H. B. *Inorg. Chem.* **1966**, *5*, 823–839.
(9) Bottomley, F.; Grein, F. *J. Chem. Soc., Dalton Trans.* **1980**, *1980*, 1359–1367.
(10) Fenske, R. R.; DeKock, R. L. *Inorg. Chem.* **1972**, *11*, 437–444. Gädeke, W.; Koch, E. E.; Dräger, G.; Frahm, R.; Saile, V. *Chem. Phys.* **1988**, *B124*, 113–119.
(11) Braga, M.; Pavao, A. C.; Leite, J. R. *Phys. Rev.* **1981**, *B23*, 4328–4336.
(12) Güida, J. A.; Aymonino, P. J.; Piro, O. E.; Castellano, E. E. *Spectrochim. Acta* **1993**, *A49*, 535–542.
(13) Pressprich, M. R.; White, M. A.; Coppens, P. *J. Am. Chem. Soc.* **1993**, *115*, 6444–6445.
(14) Rüdlinger, M.; Schefer, J.; Chevrier, G.; Furer, N.; Gudel, H. U.; Haussühl, S.; Heger, G.; Schweiss, P.; Vogt, T.; Woike, T.; Zöllner, H. *Z. Phys.* **1991**, *B83*, 125–130.
(15) Rüdlinger, M.; Schefer, J.; Vogt, T.; Woike, T.; Haussühl, S.; Zöllner, H. *Physica* **1992**, *B180 & 181*, 293–298.

0002-7863/94/1516-5233$04.50/0

frequencies of ν(NO) = 1835 cm^{-1} and ν(Fe–N) = 548 cm^{-1} for the initial photoexcited state were observed following 406-nm pulsed laser excitation of aqueous solutions of $K_2[Fe(CN)_5(NO)]$.[16] The similarity of these results to those for MS_I indicate the close association between the metastable excited states and the initial photoexcited states. The authors refer to the assignment of the absorption band at 400 nm to the 6e → 7e transition,[17] which suggests that MS_I of SNP, and presumably the excited state probed in the Raman experiment, could correspond to an electron hole in the 6e orbital, rather than in the $2b_2$ HOMO. Furthermore, the experimental Raman results were taken to imply a change in the Fe–N–O angle from linear to bent, based on interpretation of the theory for the electronic structure of nitrosyl complexes developed by Enemark and Feltham.[18] We discuss the bending of the Fe–N–O angles in both MS_I and MS_{II} in view of the current results.

Experimental Section

Sample Preparation. $Na_2[Fe(CN)_5(NO)]\cdot 2H_2O$ (Aldrich) was recrystallized from distilled water. The ground-state data were collected on an as-grown crystal. The data on the partially excited crystal were collected on a crystal cut with a silk thread saw of our own manufacture, using water as the cutting solvent. The cut (1 0 0) and ($\bar{1}$ 0 0) faces were ground smooth with sandpaper down to 0.3 μm grit. For excitation the protocol of an earlier neutron crystallography experiment[14,15] was followed. The crystal was excited with an Omnichrome series 543 argon ion laser, λ = 488 nm, polarization direction **E**//**c** and propagation direction **k**//**a**. Once a steady-state laser saturated excited-state population was obtained at 138 K, the laser was turned off, and the crystal warmed to 165 K for 5 min to eliminate the MS_{II} excited-state component and then cooled back to 138 K in preparation for X-ray data collection.

Data Collection. For both data sets X-ray intensities were measured on an Enraf-Nonius CAD4 diffractometer using graphite-monochromated Mo Kα radiation (45 kV, 32 mA). A stream of cold nitrogen gas was used to cool the crystal. The temperature was monitored throughout the experiments with a thermocouple in the cold stream, which was previously calibrated by a second thermocouple placed at the crystal position. The temperature was also monitored by periodically measuring the intensity of a relatively high angle standard reflection, (0 0 14) with (sin θ)/λ = 0.45 Å^{-1}, which was found to be insensitive to excited-state population. Reflections were selected for data collection based on two criteria: (1) their intensities had to be above a minimum threshold based on a previously reported neutron structure,[14] and (2) the X-ray beam path had to avoid the fiber supporting the crystal, which limited the accessible reflections to a hemisphere. Unit cell dimensions were obtained by a least-squares fit to the centered positions of 25 reflections with 0.34 Å^{-1} < (sin θ)/λ < 0.41 Å^{-1}.

During the mixed-states data collection the excited-state population was monitored by periodic collection of the intensities of reflections (2 1 2) and (2 3 2), which increase and decrease by 10%, respectively, upon laser saturation. The decay of the intensities of these reflections are modeled as a function of X-ray exposure time by the expression (derived in the Appendix):

$$I_H(t)/I_H(\infty) = 1 + c_H e^{-t/\tau} \qquad (2)$$

The MS_I lifetime, τ, and the coefficient, $c_H = I_H(0)/I_H(\infty) - 1$, were determined by least-squares fitting of the (2 1 2) and (2 3 2) intensities, as shown in Figure 1. The lifetime obtained, τ = 74(10) h, can be compared with a lifetime of 1.6–20 × 10^5 hours at 138 K expected for purely thermal decay using parameters obtained in a previous calorimetric study.[5] The X-ray intensity data were time-labeled for the subsequent structure factor calculation. Crystal data and X-ray data collection details are summarized in Table 1.

Data Reduction. The ground-state data were corrected for a net decay of 4% determined from a cubic polynomial fit of the periodically collected intensities of four standard reflections. For the mixed-states crystal two standards which are insensitive to the excitation, (1 0 1) and (0 0 14), showed no significant intensity change, so no correction was made for crystal decay. Corrections were made for absorption and for inhomogeneity of the incident beam.[19] The mixed-states data were not averaged because the decay of the excited state during the data collection leads to different intensities for equivalent reflections measured at different times. The variances of the mixed-states data, as determined by counting statistics, were multiplied by the sum of the number of replicates and symmetry equivalents. This procedure avoids overweighting any multiply measured unique reflection.

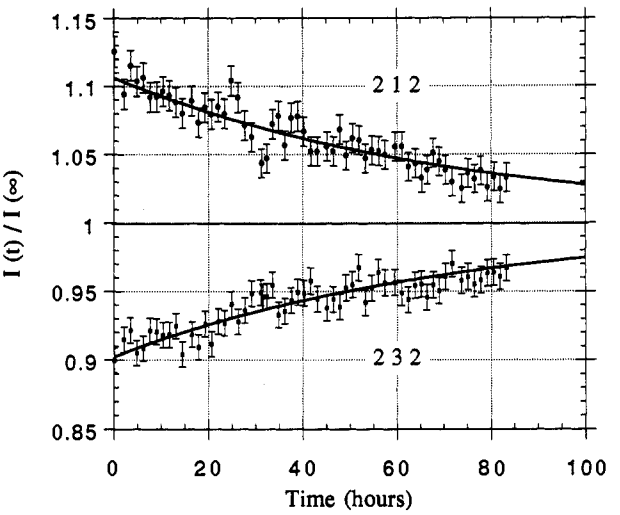

Figure 1. X-ray reflection intensity data for two standard reflections of mixed-states SNP as a function of X-ray exposure time.

Table 1. Experimental Data for $Na_2[Fe(CN)_5(NO)]\cdot 2H_2O$

	ground state	MS_I/ground state
space group	*Pnnm*	*Pnnm*
temp (K)	138 (2)	138 (2)
cell dimensions		
a (Å)	6.145(1)	6.153(1)
b (Å)	11.852(2)	11.859(3)
c (Å)	15.537(2)	15.525(3)
V (Å^3)	1131.6(3)	1132.8(4)
Z	4	4
d_{calcd} (g/cm^3)	1.749	1.751
abs coeff (cm^{-1})	14.08	14.09
cryst dimensions (mm)	0.34 × 0.18 × 0.12	0.09 × 0.41 × 0.54
radiation, wavelength (Å)	Mo Kα; λ = 0.7107	Mo Kα; λ = 0.7107
scan type	ω	ω
scan width (deg)	1.13 + 0.344 tan θ	1.13 + 0.344 tan θ
scan speed (deg/min)	0.4–5.5	0.4–5.5
$((\sin\theta)/\lambda_{min} - (\sin\theta)/\lambda_{max})$ (Å^{-1})	0.05–0.99	0.05–0.99
hkl, lower limit–upper limit	0, −22, −30; −12,22,30	0, −22, −30; −12,22,30
time period (h)	157	85
no. of std reflcns	4(1 0 1;1 2 1;0 0 4; 0 0 14)	4(1 0 1;1 2 1;0 0 4; 0 0 14)
no. of reflns measd	6722	3822
no. of symm-unique reflcns	1207	1206
no. of reflcns $F > 3\sigma(F)$	1202	1201
merging factor $R = \Sigma\|I - \langle I\rangle\|/\Sigma I$	0.016	

Structure Analysis and Multipole Refinements. Starting positions for all atoms were taken from a neutron refinement.[14,15] All least-squares refinements minimized the function $\Sigma w(|F_o|^2 - k|F_c|^2)^2$, where $w = 1/(\sigma_{counting}^2(|F|^2) + (0.01|F|^2)^2)$. Anisotropic temperature parameters were applied to all non-H atoms. Scattering factors of Fe, Na^+, O, N, C, and H were taken from ref 20. An additional parameter was included to account for extinction effects.[21] The aspherical atom multipole refinement method employed is described in ref 22. All least-squares calculations were done with either the program LSMOL or, for the mixed-states refinement, a modified version, LLSMOL, which accounts for the time dependence of the excited-state population, as described above.

For the ground-state refinement the multipole expansion was truncated at the hexadecapolar level (l = 4) for Fe and at the octapolar level (l =

(16) Yang, Y. Y.; Zink, J. I. *J. Am. Chem. Soc.* **1985**, *107*, 4799–4800. Perng, J.; Zink, J. I. *Inorg. Chem.* **1988**, *27*, 1403–1406.
(17) The numbering of the orbitals is taken from ref 8; in decreasing order of energy the ordering is 7e (LUMO), $2b_2$ (HOMO), 6e.
(18) Enemark, J. H.; Feltham, R. D. *Coord. Chem. Rev.* **1974**, *13*, 339–406.
(19) DeTitta, G. J. *J. Appl. Cryst.* **1985**, *18*, 75–79.
(20) *International Tables for X-ray Crystallography*; Kynoch: Birmingham, England, 1974; Vol. 4.
(21) Becker, P. J.; Coppens, P. *Acta Crystallogr.* **1974**, *A30*, 129–147.
(22) Hansen, N. K.; Coppens, P. *Acta Crystallogr.* **1978**, *A34*, 909–921. Li, N.; Coppens, P.; Landrum, J. *Inorg. Chem.* **1988**, *27*, 482–488.

Table 2. Summary of Least-Squares Results

	ground state	mixed states
no. of variables	148	84
$R(\|F\|)$	0.0084	0.0186
$R_w(\|F\|)$	0.0103	0.0367
$R(\|F\|^2)$	0.0144	0.0238
$R_w(\|F\|^2)$	0.0165	0.0569
GOF	1.18	1.87

3) for O, N, and C. The angular deformation of each hydrogen atom was described by a single dipole along the O–H axis. The multipole parameters were chosen assuming *pseudo*-C_{4v} symmetry for the nitroprusside dianion and C_{2v} symmetry for the water molecules. Moreover, cylindrical ($C_{\infty v}$) symmetry was imposed on the electron density of the CN and NO ligands. Expansion–contraction (κ and κ') parameters were included for the Hartree–Fock and Slater-type functions. Slater-type radial functions were used in the aspherical deformation term for all atoms except iron, for which Hartree–Fock functions were employed.

For the mixed-states refinement the atomic positions of the ground-state NP^{2-} ion were transferred from the ground-state analysis. The ground-state NP^{2-} ion was then allowed to refine as a rigid body. However, the only symmetry allowed rotational parameter, rotation about the normal to the mirror plane, was not varied as it was found to be negligible.[13] The atomic positions of the MS_INP^{2-} atoms were refined independently.

The multipole, expansion–contraction, and temperature parameters were transferred without change from the ground-state refinement to the ground-state component of the mixed-states model (initially 70% of the NP^{2-} ions and 100% of the Na^+ ions and water molecules). An additional common anisotropic temperature factor was applied to all atoms of the NP^{2-} ion to reflect the slightly different environment in the mixed-states crystal. The MS_I component, corresponding initially to 30% of the NP^{2-} ions, was constrained to have the same net temperature factors as the ground-state NP^{2-} component.

The excited NP^{2-} ion was modeled in the same way as the NP^{2-} ion in the ground-state refinement, except that the κ and κ' parameters were constrained to the ground-state values for all atoms except Fe. Variation of either or both of these parameter types for the nitroprusside ligand atoms lead to nonconvergence of the refinement.

The initially MS_I population, p_0^{exc}, in the mixed-states crystal was not refined from the X-ray data. The refinement residual, whether based on $|F|^2$ or F, is insensitive to the choice of p_0^{exc}, because a change in p_0^{exc} in the refinement leads to proportional changes in the NP^{2-} deviation from the ground-state geometry and electron density; i.e., for any geometrical or electron density deviation,

$$\Delta_i \approx \Delta_i'(p_0^{exc}/p_0^{exc'}) \tag{3}$$

This relationship is valid for all but very small (less than about 0.10) values of p_0^{exc} and has been verified for the deviation of the Fe–N bond length.[13]

The initial MS_I population was taken as derived from Mössbauer[2] and calorimetric data.[5] At 100 K, saturation of both MS_I and MS_{II} at 488 nm with the laser polarization direction **E**//**c** and the propagation direction **k**//**a** (as in the current experiment) gives a net excited population of 0.37.[2] The elimination of the fastest-decaying excited state, MS_{II}, decreases the net excited population fraction by less than 0.01, based on the ratio of excitation–enthalpies for the two states.[5] The excitation–enthalpy of the remaining state, MS_I, is temperature dependent above 120 K. With λ = 457.9 nm H_∞(138 K)/H_∞(100 K) = 0.76 and with λ = 530.9 nm the ratio is 0.89. Linear interpolation between these values gives the relevant p_0^{exc} = 0.30(2) for the wavelength of 488 nm used in the X-ray experiment.

The time dependence of the population of MS_I, $p^{excited} = p_0^{exc}\, e^{-t/\tau}$, with τ = 74 hours, was included in the calculation of the structure factors. The least-squares analyses are summarized in Table 2.

A recent polarized infrared investigation indicates that the symmetry of the MS_I/ground-state crystal may be reduced from *Pnnm* to $P2_12_12$, implying cooperative effects upon excitation.[23] Refinements including this lowering of symmetry were nonconvergent and suggest that the effect is quite small.

Theoretical Molecular Orbital Calculations. Several calculations were made with the Fenske–Hall method.[24] *Ab initio* calculations (without configuration interaction) were made with the Gaussian90 package.[25] The Dunning/Huzinaga valence double-ζ set was used for all light atoms. For Fe, an effective core potential and a double-ζ set for the valence orbitals were used.[26]

(23) Morioka, Y.; *Spectrochim. Acta*, submitted for publication.
(24) Hall, M. B.; Fenske, R. F. *Inorg. Chem.* **1972**, *11*, 768–775.

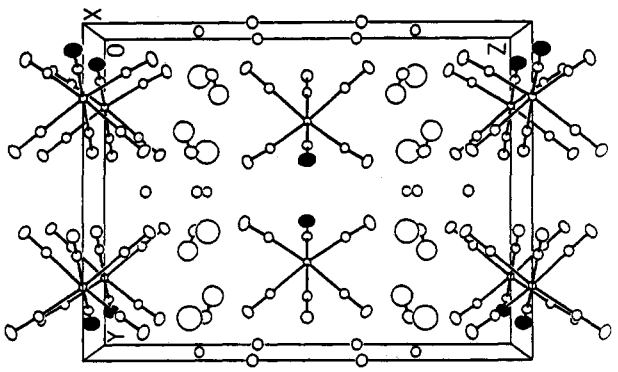

Figure 2. Packing diagram of ground-state nitroprusside at 138 K. Ellipsoids shown are 50% probability surfaces. Filled ellipsoids represent the nitrosyl group oxygen atoms.

Table 3. Atomic Fractional Coordinates and Isotropic Thermal Parameters for Ground-State SNP at 138 K

atom	x	y	z	B_{eq} (Å^2)
C(1)	0.25072(20)	0.18254(10)	0.5	0.99(4)
C(2)	0.60722(12)	0.17955(7)	0.58794(5)	0.96(4)
C(3)	0.34549(13)	0.36149(6)	0.41099(5)	1.01(3)
N(1)	0.10028(26)	0.12324(12)	0.5	1.46(3)
N(2)	0.66722(11)	0.11951(8)	0.64198(6)	1.45(4)
N(3)	0.24947(14)	0.40520(7)	0.35575(6)	1.62(3)
N(4)	0.72585(20)	0.35836(10)	0.5	0.97(3)
O(1)	0.88536(31)	0.40580(12)	0.5	1.94(4)
Fe	0.50033(3)	0.28010(1)	0.5	0.63(1)
Na(1)	0.5	0.0	0.24575(2)	1.07(1)
Na(2)	0.0	0.0	0.37802(3)	1.27(1)
O(2)	0.17239(14)	0.12246(8)	0.26867(5)	1.69(5)
H(1)	0.185(3)	0.177(3)	0.281(1)	2.1(8)
H(2)	0.095(4)	0.122(2)	0.239(2)	2.1(8)

Results

Description of the Ground-State Structure. The current results for the geometry of the SNP ground state are in good agreemewnt with those of previous studies.[14,15,27,28] The unit cell contents are shown in Figure 2. The positional parameters and isotropic thermal parameters are listed in Table 3, while bond lengths and angles are presented in Table 4. Multipole populations and expansion–contraction parameters are available as supplementary material.

Dynamic deformation density maps for the ground state, included in the supplementary material, are similar to those published by Antipin et al.[28] Static deformation density maps are shown in Figure 3. The map of the equatorial plane (Figure 3a) shows an accumulation of density along the *xy* diagonals. A section through an axial plane (Figure 3b) shows significant density between Fe and the NO ligand, as expected for a strong, significantly covalent, bond.

The populations of the d-orbitals derived from the Fe multipoles[29] are compared in Table 5 with theoretical Mulliken

(25) Gaussian 90, Revision J; Frisch, M. J.; Head-Gordon, M.; Trucks, G. W.; Foresman, J. B.; Schlegel, H. B.; Raghavachari, K.; Robb, M.; Binkley, J. S.; Gonzalez, C.; Defrees, D. J.; Fox, D. J.; Whiteside, R. A.; Seeger, R.; Melius, C. F.; Baker, J.; Martin, R. L.; Kahn, L. R.; Stewart, J. J. P.; Topiol, S.; Pople, J. A. Gaussian Inc.; Pittsburgh, PA, 1990.
(26) Hay, P. J.; Wadt, W. R. *J. Chem. Phys.* **1985**, *82*, 270–283. Wadt, W. R.; Hay, P. J. *J. Chem. Phys.* **1985**, *82*, 284–298. Hay, P. J.; Wadt, W. R. *J. Chem. Phys.* **1985**, *82*, 299–310.
(27) Bottomley, F.; White, P. S. *Acta. Crystallogr.* **1979**, *B35*, 2193–2195. Navaza, A.; Chevrier, G.; Alzari, P. M.; Aymonino, P. J. *Acta Crystallogr.* **1989**, *C45*, 839–841.
(28) Antipin, M. Yu.; Tsirel'son, V. G.; Flyugge, M. P.; Stuchkov, Yu. T.; Ozerov, R. P. *Sov. J. Coord. Chem.* **1987**, *13*, 67–75.
(29) Holladay, A.; Leung, P. C.; Coppens, P. *Acta Crystallogr.* **1983**, *A39*, 377–387.

Table 4. Bond Lengths and Angles for Ground State and MS_1 SNP at 138 K[a]

distance	ground state	excited state
Fe–N(4)	1.668(1)	1.717(8)
Fe–C(1)	1.921(1)	1.904(10)
Fe–C(2)	1.928(1)	1.930(6)
Fe–C(3)	1.936(1)	1.927(6)
N(4)–O(1)	1.129(2)	1.130(13)
C(1)–N(1)	1.161(2)	1.160(14)
C(2)–N(2)	1.161(1)	1.140(9)
C(3)–N(3)	1.163(1)	1.167(10)
angle	**ground state**	**excited state**
C(1)–Fe–C(2)	84.26(3)	85.0(3)
C(1)–Fe–C(3)	84.69(3)	85.5(3)
C(1)–Fe–N(4)	176.78(6)	177.4(4)
C(2)–Fe–C(2a)[b]	90.23(3)	90.1(3)
C(2)–Fe–C(3)	168.94(3)	170.5(3)
C(2)–Fe–C(3a)[b]	88.23(3)	88.7(3)
C(2)–Fe–N(4)	93.48(4)	93.2(3)
C(3)–Fe–C(3a)[b]	91.17(3)	90.9(3)
C(3)–Fe–N(4)	97.54(4)	96.3(3)
Fe–C(1)–N(1)	179.77(12)	179.7(6)
Fe–C(2)–N(2)	178.41(7)	178.1(6)
Fe–C(3)–N(3)	176.56(7)	176.6(6)
Fe–N(4)–O(1)	175.93(13)	173.6(8)

[a] Distances are in Å and angles are in deg. [b] C(2a) and C(3a) are related to C(2) and C(3) by a crystallographic mirror plane at $z = 0.5$.

populations from the Fenske–Hall calculation and populations as defined by Larsson[30] from a multiple-scattering calculation.[11] The Fenske–Hall results are in good agreement with previous calculations for the frontier (HOMO and LUMO) orbitals.[8,10,11] The theoretical and experimental d-orbital results indicate that the ground-state d-orbital populations increase in the order $z^2 < x^2-y^2 < xz, yz < xy$, as expected from simple crystal field considerations.

The atomic character of the frontier orbitals from our *ab initio* calculations is in essential agreement with previous INDO results.[9] However, the symmetry of the HOMO from this calculation does not agree with conclusions based on experiment, which are confirmed by the Fenske–Hall calculation and previously reported theoretical results.[8,10,11] Polarized absorption,[8] photoelectron and XANES spectroscopy[31] indicate that the HOMO has $a'(b_2)$ symmetry, but according to the *ab initio* calculation the highest energy, occupied $a'(b_2)$ orbital lies 1.5 eV below the calculated HOMO level. As the experimental conclusions seem unambiguous, we have not used the *ab initio* results.

The Fenske–Hall results are therefore used for comparison in the following discussion.

Description of the MS_1 structure. The refinement of the ground-state NP^{2-} anion in the mixed-states crystal as a rigid body yielded negligible translational shifts (Δx = –0.0010(8)Å and Δy = –0.0014(5)Å). Bond lengths and angles for the MS_1 nitroprusside ion are included in Table 4, and coordinates are listed in Table 6.

The distortion of the excited nitroprusside ion from its ground-state geometry is best described with reference to Figure 4, in which the ground-state and the excited-state ion with displacements, exaggerated by a factor of 10, are shown superimposed. The statistically significant geometrical distortions ($\Delta_i > 3\sigma(\Delta_i)$) of MS_1 relative to the ground state are an elongation of the Fe–N bond by 0.049(8) Å from 1.668(1) Å to 1.717(8) Å, and a decrease in the average *cis* ∠N–Fe–C angle by 0.8(2)° from 95.51(3)° to 94.75(19)°. Since the excited-state population at the start of the X-ray data collection is 30(2)%, a one standard deviation difference in the population corresponds to the range 0.045(7)Å ≤ Δ(Fe–N) ≤ 0.053(9) Å. In the ground state the iron atom is 0.186 Å above the plane of the equatorial ligands, compared to 0.160 Å in the excited state. The change in the Fe–N–O angle is not statistically significant, in agreement with polarized light studies reported in ref 12. The geometry changes between the ground state and MS_1 are summarized in Table 7.

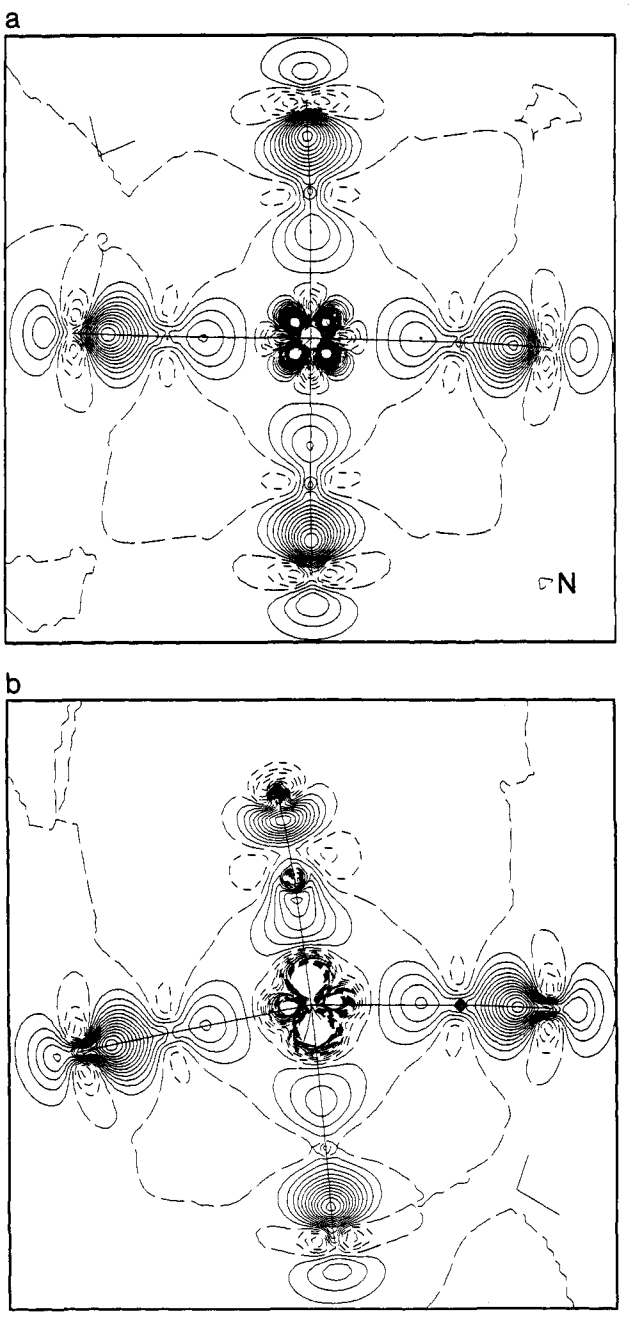

Figure 3. Static deformation density maps for ground-state SNP. Parts a and b show planes containing the equatorial and axial ligands, respectively. The axial plane also includes two of the equatorial ligands. The nitrosyl ligand is at the top of part b. Contour lines are at 0.05 e/Å^3 intervals.

Table 5. d-Electron Orbital Populations[a]

	experimental		theoretical			
orbital	gs	es	gs (FH)	gs (MS)[b]	es[c]	spherical[d]
d_{z^2}	0.14(7)	2.0(5)	1.09	0.66	1.08	1.20
$d_{x^2-y^2}$	0.98(7)	1.8(5)	1.17	0.56	1.17	1.20
d_{xz}	1.09(4)	1.9(3)	1.36	1.47	1.47	1.20
d_{yz}	1.09(4)	1.9(3)	1.36	1.47	1.47	1.20
d_{xy}	1.91(7)	–1.9(5)	1.78	1.82	0.94	1.20

[a] Abbreviations: gs, ground state; es, excited state; FH = Fenske–Hall, MS = multiple scattering. [b] Reference 11. [c] As estimated from a Fenske–Hall ground-state calculation, using the excited-state geometry, by promoting one electron from the HOMO to the LUMO. [d] Assuming Fe(II).

(30) Larsson, S. *Theor. Chim. Acta* **1978**, *49*, 45.
(31) Gädeke, W.; Koch, E. E.; Dräger, G.; Frahm, R.; Saile, V. *Chem. Physics* **1988**, *124*, 113–119.

Table 6. Atomic Fractional Coordinates and Isotropic Thermal Parameters for the Excited-State SNP Ion and Na^+ and H_2O Atoms in the Mixed-States Crystal at 138 K

atom	x	y	z	B_{eq} (Å^2)
C(1e)	0.2459(16)	0.1818(8)	0.5	0.99(4)
C(2e)	0.6039(10)	0.1780(5)	0.5880(4)	0.97(4)
C(3e)	0.3436(10)	0.3610(5)	0.4116(4)	1.01(4)
N(1e)	0.0953(17)	0.1228(8)	0.5	1.47(4)
N(2e)	0.6652(10)	0.1204(5)	0.6415(5)	1.46(4)
N(3e)	0.2481(11)	0.4063(6)	0.3566(5)	1.63(4)
N(4e)	0.7253(13)	0.3593(6)	0.5	0.97(4)
O(1e)	0.8880(18)	0.4037(7)	0.5	1.95(4)
Fe(e)	0.4941(5)	0.2779(2)	0.5	0.63(1)
Na(1)	0.5	0.0	0.24573(4)	1.06(2)
Na(2)	0.0	0.0	0.37792(4)	1.25(2)
O(2)	0.17304(17)	0.12197(9)	0.26874(7)	1.65(4)
H(1)	0.1883(13)	0.1774(6)	0.2810(5)	2.1(8)
H(2)	0.0968(12)	0.1236(6)	0.2385(5)	2.1(8)

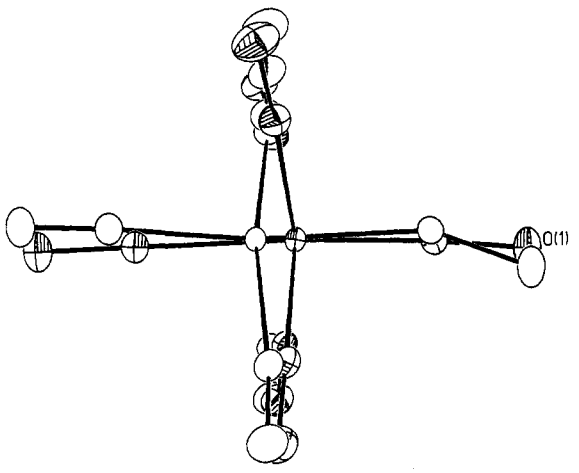

Figure 4. Superimposed thermal ellipsoid plots of the ground (shaded ellipsoids) and MS_I (open ellipsoids) nitroprusside ions. The crystallographic c axis is normal to the page. Distortions upon excitation have been exaggerated by a factor of 10.

The experimental and theoretical d-orbital populations for the excited state are included in Table 5. The nonphysical, negative, d_{xy} population shows that the experimental MS_I electron density results should be regarded in only a qualitative manner, though the depletion of the d_{xy} orbital is in agreement with the theoretical values. It is graphically apparent in Figure 5 which shows the static deformation density maps for the ground state and MS_I. Multipole populations and expansion–contraction parameters are listed in the supplementary material.

Discussion

The previously reported results for the MS_I distortion from a neutron investigation are generally confirmed.[14,15] Obviously, the inference made in the neutron study regarding the deviation of the actual distortion from the refined average MS_I/ground-state structure (expression 1) leads to reasonable results, and allows direct comparison of the X-ray and neutron results once a small discrepancy in the assumed initial excited-state population is resolved.[32] The agreement is rather good (Table 7), though the accuracy of the neutron results may be affected by the use of thermal parameters to describe the superposition of two different species in one crystal.

The elongation of the iron–nitrosyl bond following excitation agrees with the promotion of an electron into the ground-state LUMO (e), which is primarly d_{xz}, d_{yz}, and π^*(NO) in character. The LUMO is antibonding with respect to both the Fe–N and N–O bonds, so its occupation leads to a lengthening of both bonds. This is observed for Fe–N and N–O, although the N–O bond length increase is not statistically significant ($\Delta l_{NO} < 3\sigma(\Delta l_{NO})$). The decrease in the ∠N–Fe–C angle is understood as a minimization of ligand–ligand repulsion associated with the elongation of the Fe–N bond, which leaves the average axial–ligand to equatorial–ligand distances almost unchanged (the average C_{ax} to C_{eq} distance increases by 0.005(6) Å and the average nitrosyl N to C_{eq} distance increases by 0.016(7) Å). The significant decrease in d_{xy} electron density indicates that MS_I originates from the partial depopulation of the ground-state HOMO ($2b_2$).

Table 7. Geometric Differences between MS_I and Ground-State Nitroprusside

distance	X-ray results (this study)	reanalysis[a] of neutron results[14,15]
Fe–N(4)	0.049(8)	0.051(6)
Fe–C(1)	–0.017(10)	–0.031(5)
Fe–C(2)	0.002(6)	–0.009(5)
Fe–C(3)	–0.009(6)	0.001(5)
N(4)–O(1)	0.001(13)	0.009(8)
C(1)–N(1)	–0.001(14)	–0.005(8)
C(2)–N(2)	–0.021(9)	0.008(5)
C(3)–N(3)	0.004(10)	0.001(5)
angle	**X-ray results (this study)**	**reanalysis[a] of neutron results[14,15]**
C(1)–Fe–C(2)	0.7(3)	0.8(2)
C(1)–Fe–C(3)	0.8(3)	1.1(2)
C(1)–Fe–N(4)	0.6(4)	0.5(4)
C(2)–Fe–C(2a)[b]	–0.1(3)	
C(2)–Fe–C(3)	1.6(3)	2.0(3)
C(2)–Fe–C(3a)[b]	0.5(3)	0.2(2)
C(2)–Fe–N(4)	–0.3(3)	–0.5(3)
C(3)–Fe–C(3a)[b]	–0.3(3)	
C(3)–Fe–N(4)	–1.2(3)	–1.5(2)
Fe–C(1)–N(1)	–0.7(6)	
Fe–C(2)–N(2)	–0.3(6)	
Fe–C(3)–N(3)	0.0(6)	
Fe–N(4)–O(1)	–2.3(8)	–0.2(6)

[a] The parameter differences and esd's from ref 12 have been multiplied by 1/0.37, corresponding to the expected 0.37 fractional population for the neutron experiment excitation method.[2,14,15] [b] C(2a) and C(3a) are related to C(2) and C(3) by an xy mirror plane at z = 0.5.

The excited state formed following a $b_2 \rightarrow e$ transition for SNP has E symmetry. A Jahn–Teller distortion of this degenerate state lifts the degeneracy and leads to a bent Fe–N–O angle. Whether or not Jahn–Teller or crystal packing effects are dominant in controlling the Fe–N–O angle in SNP, the slight bend of the Fe–N–O angle in both the ground and the MS_I excited states implies that the LUMO splits into a′ and a″ components in the C_s symmetry. Given that MS_I and MS_{II} are maximally populated[32] when **E** is respectively parallel and perpendicular to the mirror plane,[5,33] it seems reasonable to assign MS_I and MS_{II} as relaxed derivatives of the excited configurations a′ $(2b_2)^1$a″ $(7e)^1$ and a′ $(2b_2)^1$a′ $(7e)^1$, respectively, in accordance with C_s symmetry electric dipole transition requirements.

According to the electronic level diagram of nitrosyl complexes of Enemark and Feltham,[17] these assignments imply bending for the lower energy state (MS_{II}) and linearity for the higher energy state (MS_I), in the absence of external forces. This is illustrated for nitroprusside in Figure 6. The observed near-linearity of MS_I is therefore as theoretically expected, though crystal packing effects may also contribute. A recent neutron investigation indicates near-linearity for MS_{II} also, in apparent contradiction with theory, but possibly a result of crystal packing effects.

The observed increase in the d_{z^2} orbital population in MS_I is difficult to correlate with the structural results. Population of the empty $\sigma^*(d_{z^2})$ orbital should lead to a weakening of the trans metal–ligand bond,[34] which is supported by the observed dis-

(32) At 100 K, saturation of both MS_I and MS_{II} at 488 nm with **E**//**c** and **k**//**a** gives a net excited population of 0.37 according to a Mössbauer study.[2] As the neutron study was performed under these experimental conditions, it is not clear to us why a value of 0.45 was assumed instead. In our reanalysis of the neutron data we assume the former value.

(33) Zöllner, H. Jülich Report *2332*, Jülich, Germany, 1989.

(34) Richter-Addo, G. B.; Legzdins, P. *Metal Nitrosyls*; Oxford University Press: 1992.

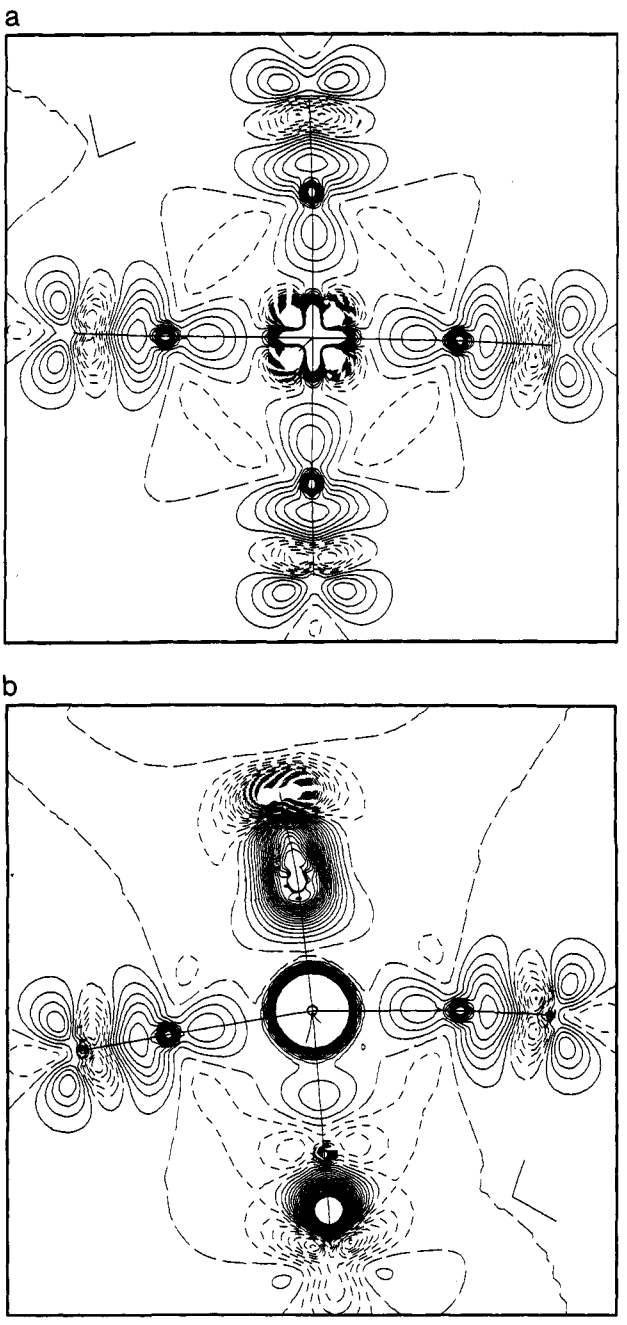

Figure 5. Static deformation density maps for MS_I SNP. Parts a and b show the same planes as Figure 3 (parts a and b, respectively). Contours as in Figure 3.

sociation of a cyanide ligand on $1e^-$ reduction of NP^{2-} in aqueous solution.[35] However, we observe no significant bond length increase for axial Fe–CN in the present study.

Conclusions

Following excitation of the nitroprusside ion and transition to the MS_I state, the Fe–N bond length increases by 0.049(8) Å, and the average *cis*∠N–Fe–C angle decreases by 0.8(2)°. These distortions are in agreement with charge transfer from an orbital of primarily Fe character to the anti-bonding LUMO, followed by a relaxation which minimizes ligand–ligand repulsion. A comparison of experimental electron densities for the ground state and MS_I indicates significant depletion of the d_{xy} orbital, in agreement with the formation of an electron hole in the $2b_2$ HOMO rather than in the lower energy 6e orbital. On the basis of these geometry and electron density changes as well as previously reported polarization results,[5,33] MS_I is assigned as a relaxed derivative of the $a'\ (2b_2)^2\ a''\ (7e)^0 \rightarrow a'\ (2b_2)^1 a''\ (7e)^1$ photoexcited state. The lack of appreciable bending of the ∠Fe–N–O angle in MS_I agrees with the accepted electronic structure of nitrosyl complexes, though the near-linearity observed for MS_{II}[15] suggests that packing forces in the crystals also contribute.

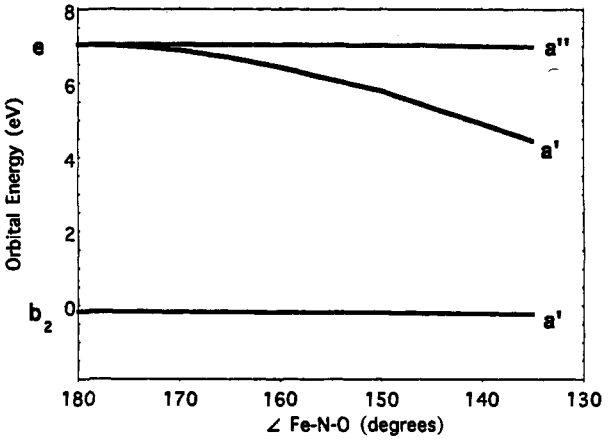

Figure 6. Frontier orbitals of the nitroprusside dianion. The ion has been constrained to C_{4v} symmetry except for the Fe–N–O angle.

Acknowledgment. We thank Professors Frank V. Bright and Athos Petrou of SUNY/Buffalo for the use of their equipment and for their helpful advice and Dr. Mogens S. Lehmann of the Institut Laue-Langevin for bringing the metastable states of SNP to our attention. Acknowledgement is made to the donors of The Petroleum Research Fund, administered by the American Chemical Society (PRF26119-AC6,3), for partial support of this research. Support of this work by the National Science Foundation (CHE9021069) is gratefully acknowledged.

Appendix: Structure Factor Expression for a Decaying Excited State

Assuming coherent scattering, the structure factor can be expressed as

$$F(\mathbf{H}) = F_g(\mathbf{H}) + p\Delta F(\mathbf{H}) \qquad \text{(A1)}$$

where p is the excited-state population. For a time dependence of the population described by $p = p_0 e^{-t/\tau}$, the intensity will not have a simple, single exponential form because of the appearance of both squared and cross-terms in the expression for $|F|^2 \propto I$. However, for small $p|\Delta F|$, the time dependence of the intensity of a reflection can be approximated as

$$I(t) = I_g + \Delta I e^{-t/\tau} \qquad \text{(A2)}$$

Equation 2 in the Experimental Section is equivalent to this expression since $I(t = \infty) = I_g$.

Supplementary Material Available: Anisotropic thermal, multipole population, and expansion–contraction parameters and dynamic deformation density maps of the equatorial and an axial plane of the ground state (4 pages); listings of observed and calculated structure factors for the ground-state and the mixed-states crystals (147 pages). This material is contained in many libraries on microfiche, immediately follows this article in the microfilm version of the journal, and can be ordered from the ACS; see any current masthead page for ordering information.

(35) Glidewell, C.; Johnson, I. L. *Inorg. Chim. Acta* **1987**, *132*, 145–147.